Spinel-Corundum Equilibria and Activities in the System MgO-Al$_2$O$_3$-Cr$_2$O$_3$ at 1473 K

K.T. JACOB and C.K. BEHERA

The tie-lines delineating intercrystalline ion-exchange equilibria between MgAl$_2$O$_4$-MgCr$_2$O$_4$ spinel solid solution and Al$_2$O$_3$-Cr$_2$O$_3$ solid solution with corundum structure have been determined at 1473 K by electron microprobe and X-ray diffraction (XRD) analysis of equilibrated phases. The tie-lines are skewed to the solid solution 0.7MgAl$_2$O$_4$-0.3MgCr$_2$O$_4$. The lattice parameters and molar volumes of both the solid solution series exhibit positive deviations from Vegard's and Retger's laws, respectively. Activities in the spinel solid solution are derived from the tie-line information and thermodynamic data on Al$_2$O$_3$-Cr$_2$O$_3$ solid solution available in the literature. Activities of Mg$_{0.5}$CrO$_2$ and Mg$_{0.5}$AlO$_2$ in the spinel solid solution exhibit strong positive deviations from Raoult's law over most of the composition range. However, activity of Mg$_{0.5}$CrO$_2$ exhibits mild negative deviation for compositions rich in Mg$_{0.5}$CrO$_2$. The activity-composition relationship in the spinel solid solution is analyzed in terms of the intracrystalline exchange of cations between the tetrahedral and octahedral sites of the spinel structure. The intracrystalline ion exchange is governed by site preference energies of the cations. The difference between the Gibbs energy of mixing calculated using the cation mixing model and the experimental data is taken as a measure of the strain contribution arising from the difference in the radii of Al^{3+} and Cr^{3+} ions. The large positive strain enthalpy suggests the onset of immiscibility in the spinel solid solution at low temperatures. The computed critical temperature and composition for phase separation are 802 ($\pm$20) K and $X_{MgCr_2O_4} = 0.46$ ($\pm$0.02), respectively.

I. INTRODUCTION

RECENTLY several attempts have been made to produce crude molten stainless steel by direct smelting of iron-chromium ore in a basic oxygen furnace (BOF), without the use of ferrochromium alloys, in order to save electrical energy and reduce the cost of production.[1–4] Some fundamental studies on the reduction rate of solid chromium ore and kinetics of smelting reduction of chromium ore by carbonaceous materials have been conducted.[5–9] However, there is limited thermodynamic data on the complex ores used. For a better understanding of the new process, especially the reduction stage, it is useful to have good data on the starting material. It is known that iron-chromium ore generally consists of a spinel solid solution containing Fe$_3$O$_4$, FeAl$_2$O$_4$, FeCr$_2$O$_4$, MgAl$_2$O$_4$, and MgCr$_2$O$_4$. Since Fe$_3$O$_4$ in the ore can be easily reduced by solid carbon or reducing gas, iron-chromium ore after initial reduction is essentially a spinel solid solution (Fe,Mg)(Al, Cr)$_2$O$_4$. The solid solution on further reduction can give a mixture of Fe-Cr alloy, a spinel solid solution Mg(Al,Cr)$_2$O$_4$, and a sesquioxide solid solution (Al,Cr)$_2$O$_3$.

As a part of systematic studies on the complex spinel solid solutions, measurements have been made on the system MgO-Al$_2$O$_3$-Cr$_2$O$_3$ at 1473 K. Tie-lines connecting the spinel solid solution MgAl$_2$O$_4$-MgCr$_2$O$_4$ and the corundum solid solution Al$_2$O$_3$-Cr$_2$O$_3$ were determined experimentally. The activities and mixing properties of the spinel solid solution

are derived from the tie-line data. In earlier studies,[10,11] activities in the spinel solid solution FeAl$_2$O$_4$-FeCr$_2$O$_4$ have been measured as a function of temperature and composition using electromotive force and phase equilibrium techniques. The main contributions to the Gibbs energy of mixing are the configurational entropy from mixing of cations on tetrahedral and octahedral sites and strain enthalpy due to size difference between Al^{3+} and Cr^{3+} ions. More recently, activities of the constituents in the FeAl$_2$O$_4$-MgAl$_2$O$_4$ and FeCr$_2$O$_4$-MgCr$_2$O$_4$ solid solutions were investigated using a solid-state cell in the temperature range 1100 to 1350 K.[12,13] Mild negative deviations from Raoult's law were observed. The mixing properties for both systems were adequately represented by a regular solution model. Values of the regular solution parameter, defined by $\Omega = \Delta H/X(1 - X) = \Delta G^E/X(1 - X)$, are -1.9 ($\pm$0.17) kJ mol^{-1} for the Fe$_X$Mg$_{1-X}$Al$_2$O$_4$ solid solution and -2.26 ($\pm$0.20) kJ mol^{-1} for the Fe$_X$Mg$_{1-X}$Cr$_2$O$_4$ solid solution. The thermodynamic behavior of the two solid solution series is mainly influenced by mixing of the divalent cations on the tetrahedral sites.

The activity of MgCr$_2$O$_4$ in the spinel solid solution MgAl$_{1-X}$Cr$_X$O$_4$ was measured by Morita et al.[14] by equilibrating the solid solution with MgO and Ni-Cr alloys under controlled oxygen potentials. Although the data show significant scatter, the results indicate negative deviation from Raoult's law. Hino et al.[15] have located three tie-lines between the spinel and corundum solid solutions in the system MgO-Al$_2$O$_3$-Cr$_2$O$_3$ at 1573 K. However, the data are insufficient to derive activity-composition relations in the spinel solid solution. The molar volume of mixing of the spinel solid solution can be expressed as $\Delta V^M = X_{MgAl_2O_4}X_{MgCr_2O_4} (0.423 - 0.209 X_{MgCr_2O_4})$ cm^3 mol^{-1}. The corresponding expression for the solid solution Al$_2$O$_3$-Cr$_2$O$_3$ with corundum structure is $\Delta V^M = X_{Al_2O_3}X_{Cr_2O_3} (0.4627 -$

K.T. JACOB, Professor, Department of Metallurgy and Materials Researcher Center, and C.K. BEHERA, Graduate Student, Department of Metallurgy, are with the Indian Institute of Science, Bangalore, 560 012, India.
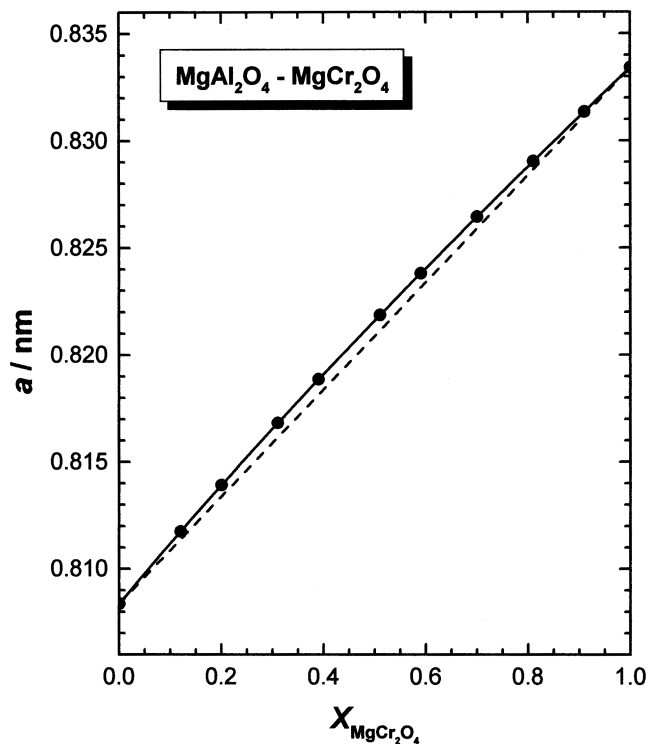
Fig. 1—Variation of the lattice parameter of the spinel solid solution $MgAl_2O_4$-$MgCr_2O_4$ with composition. The samples were quenched from 1300 K.

Fig. 2—Variation of the lattice parameter with composition of Al_2O_3-Cr_2O_3 solid solution with corundum structure. The samples were quenched from 1300 K.

0.1355 $X_{Cr_2O_3}$) cm^3 mol^{-1}. The volume of mixing of the sesquioxide solid solution is ~24 pct larger than that for the spinel solid solution.

II. EXPERIMENTAL TECHINQUE

A. *Materials*

The Al_2O_3-Cr_2O_3 solid solutions were prepared by mixing powders of 99.99 pct pure component oxides in the required ratio, compacting the mixture into pellets, and heating at 1873 K for a total period of 9 days in a stream of dry argon gas. The pellet was crushed and repelletized twice during this period. Magnesium aluminate ($MgAl_2O_4$) and magnesium chromite ($MgCr_2O_4$) were prepared by heating pellets of $MgO + Al_2O_3$ and $MgO + Cr_2O_3$, respectively, in the required molar ratio at 1500 K for 6 days in argon gas. Spinel solid solutions were prepared in a similar manner starting from the pure spinel compounds. However, after the initial treatment, the materials were crushed, repelletized, resealed, and equilibrated at 1500 K for an additional 6 days. The formation of spinel compounds and homogeneous solid solutions was confirmed by powder X-ray diffraction (XRD). The lattice parameters of both spinel and corundum solid solutions were determined after quenching from 1300 K. The lattice parameters were found to exhibit positive deviation from Vegard's law, as shown in Figures 1 and 2. For the solid solution with corundum structure (space group $R\bar{3}c$), the *a* parameter exhibits larger deviation from Vegard's law than the *c* parameter. The results obtained in this study contrast sharply with the data of Tsai and Muan,[16] who reported negative deviation for d_{116} as a function of composition. Figures 1 and 2 were used as calibration standards to
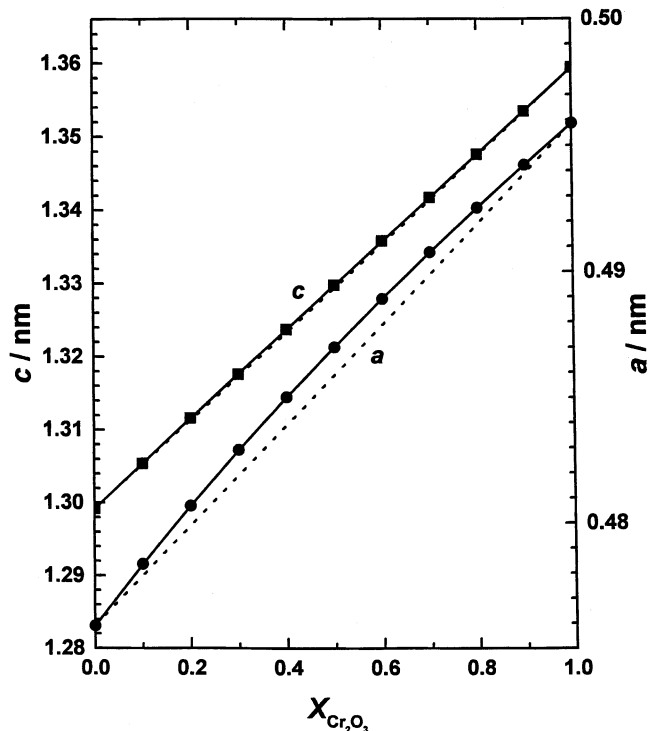
derive unknown compositions of the solid solution phases in equilibrated samples from their measured lattice parameters. The molar volumes of the two solid solutions also exhibit positive deviations from ideal behavior (Retger's law), as shown in Figures 3 and 4, respectively. The molar volumes deviate less from linear behavior than the lattice parameters.

B. *Apparatus and Procedure*

Powders of spinel solid solution (average particle size ~7 μm) and sesquioxide solid solution (~1 μm) were intimately mixed in the molar ratio 3:2 and then pelletized. Preliminary experiments indicated that the composition of the spinel grains approached equilibrium faster than the grains of the sesquioxide. Interdiffusion of cations in the spinel solid solution appeared to be more rapid than that in the corundum solid solution. Hence, smaller particles of the corundum phase and an excess of spinel phase were taken to achieve equilibrium intercrystalline partitioning of cations more rapidly. The chromium/aluminum molar ratio of the starting solid solutions in each pellet were approximately equal. The pellets were placed in alumina crucibles and heated at 1473 K for 7 days under flowing argon gas. At the end of this period, the capsules were quenched. The material was reground, repelletized, and heated for another 7 days under identical conditions. Following the second quench, the pellets were mounted for metallographic examination and composition analysis of the spinel phase using electron microprobe analysis (EPMA). Pure MgO, Al_2O_3, and Cr_2O_3 were used as standards. In all cases, atomic absorption and fluorescence effects were eliminated using computer-compensated adjustments (ZAF). The composition profiles across the spinel grains were found to be uniform. The spinel phase near the $MgAl_2O_4$ side in equilibrium
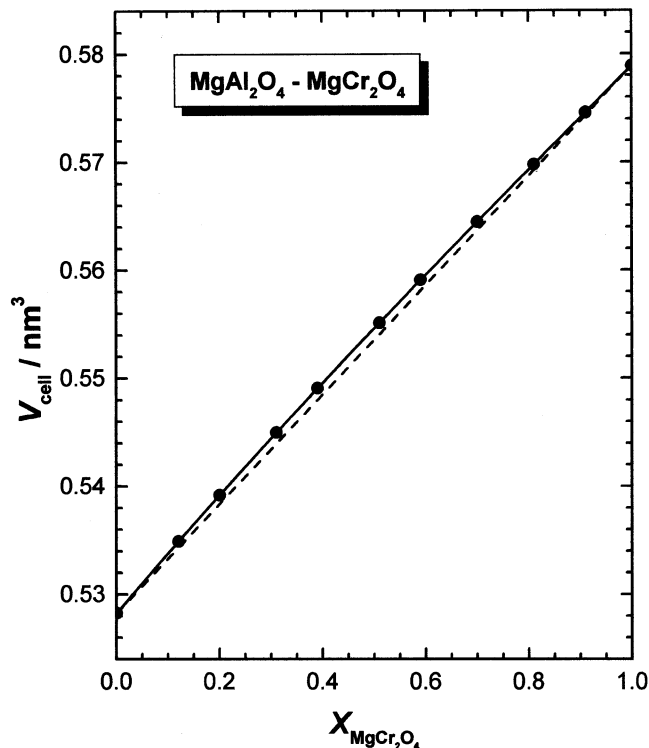
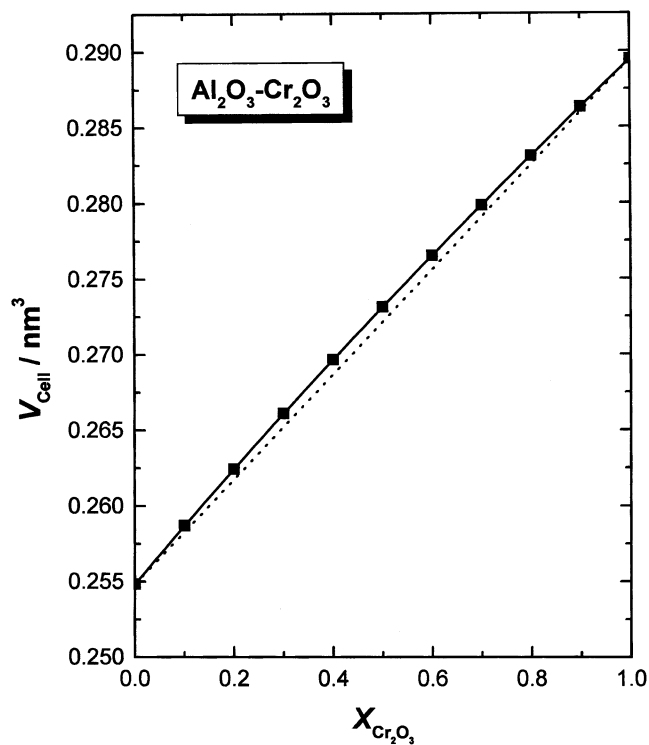Fig. 3—Variation of unit cell volume of the spinel solid solution $MgAl_2O_4$-$MgCr_2O_4$ with composition.

Fig. 4—Variation of unit cell volume of the solid solution Al_2O_3-Cr_2O_3 with corundum structure as a function of composition.

with the corundum solid solution was nonstoichiometric, with a small excess of the sesquioxide phase. Pure $MgAl_2O_4$ in equilibrium with α-Al_2O_3 contained 51.8 (±0.5) mol pct

Table I. Tie-Line Compositions of $Mg(Al,Cr)_2O_4$ and $(Al,Cr)_2O_3$ Solid Solutions at 1473 K

Composition of Corundum Solid Solution, $X_{CrO_{1.5}}$ or $X_{Cr_2O_3}$	Composition of Spinel Solid Solution, $X_{Mg_{0.5}CrO_2}$ or $X_{MgCr_2O_4}$
0.048	0.146
0.114	0.330
0.193	0.494
0.275	0.572
0.356	0.607
0.421	0.621
0.504	0.639
0.580	0.655
0.663	0.691
0.739	0.721
0.816	0.763
0.905	0.830
0.960	0.903

Al_2O_3. The composition of the small corundum grains could not be determined accurately by EPMA. Lattice parameters of the equilibrated samples determined by XRD were used to obtain the composition of the corundum phase. For the spinel phase, the composition determined from the lattice parameters agreed within 2 pct with that determined by EPMA. In view of the small deviation of the spinel phase from stoichiometry near the $MgAl_2O_4$-rich side, the EPMA results are considered to be more accurate. The reversibility of the Al-Cr exchange between the two solid solutions was established by the familiar "tie-line rotation" technique. Any composition in the two-phase region of the ternary triangle can be prepared by taking different compositions of the spinel and corundum solid solutions. During equilibration, the line joining the initial compositions of the two phases will rotate about the mean composition to its equilibrium tie-line position. By choosing appropriate initial compositions of the two solid solutions, the lines joining them can be made to rotate in opposite directions. When both clockwise and counterclockwise rotations result in the same final position after equilibration, establishment of equilibrium is confirmed.

III. RESULTS

Tie-Line Study

The equilibrium compositions of $Mg(Al,Cr)_2O_4$ and $(Al,Cr)_2O_3$ solid solutions at 1473 K are given in Table I. The corresponding tie-lines are displayed in Figure 5. The tie-lines are slightly skewed toward the $MgCr_2O_4$ corner. Three tie-lines determined by Hino et al.[15] at 1573 K are shown for comparison. The tie-line of Hino et al. near the Al_2O_3-rich side is almost parallel to that obtained in this study. The directions of the other two tie-lines are quite different from those obtained in this study. Hino et al. determined the composition of the corundum solid solution from XRD using the incorrect data of Tsai and Muan[16] on the variation of d_{116} with composition. This probably led to an incorrect evaluation of composition of the sesquioxide phase.

The relation between the equilibrium compositions of the two solid solutions at 1473 K is shown in Figure 6. The continuous curve is obtained, with the slope first decreasing with $X_{Cr_2O_3}$ and then increasing again. The intercrystalline

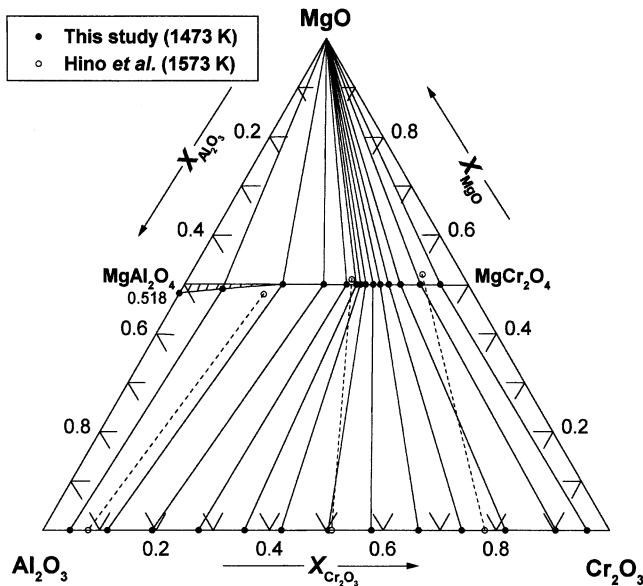Fig. 5—Isothermal section of the phase diagram for the system MgO-Al_2O_3-Cr_2O_3 at 1473 K. Tie-lines connecting solid solution with spinel and corundum structures determined in this study at 1473 K are compared with the data of Hino et al.[15] at 1573 K.
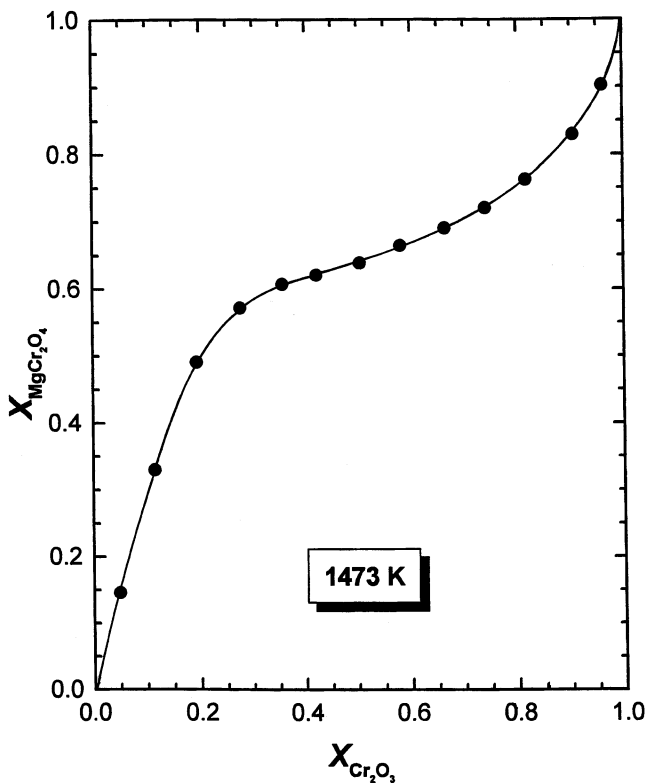

Fig. 6—Equilibrium relation between mole fractions of $MgCr_2O_4$ in the spinel solid solution and Cr_2O_3 in the corundum solid solution at 1473 K.

ion exchange equilibrium between the solid solutions having spinel and corundum structures can be represented by the equation

$$Cr_2O_3 + MgAl_2O_4 \rightarrow Al_2O_3 + MgCr_2O_4 \quad [1]$$

The formation of the solid solution between magnesium

aluminate and magnesium chromite involves the mixing of two Al^{3+} and Cr^{3+} ions per formula unit. The other ions are common. $MgAl_2O_4$ and $MgCr_2O_4$ are both normal spinels at low temperature and, as will be shown later, the trivalent ions are predominantly confined to octahedral sites at 1473 K. It is more appropriate, therefore, to express activities and mixing properties of the spinel solid solutions in terms of one mole of the mixing species. Following Kerric and Darken,[17] the composition variables are expressed as $Mg_{0.5}AlO_2$ and $Mg_{0.5}CrO_2$. With this choice of composition variables, the logarithm of the activity coefficients will always have a finite value and will not go to minus infinity as the concentration approaches zero. The corresponding composition variables for the corundum solid solution are $AlO_{1.5}$ and $CrO_{1.5}$.

When the tie-lines between two solid solution phases are known and activity data for one phase are available, the activities of the components in second phase can be calculated. This is accomplished using a modified Gibbs–Duhem integration technique proposed by Jacob and Jeffes.[18]

$$\log \gamma_{Mg_{0.5}CrO_2} = - \int_1^{X_{Mg_{0.5}CrO_2}} X_{Mg_{0.5}AlO_2} \, d$$

$$\log \frac{a_{AlO_{1.5}} X_{Mg_{0.5}CrO_2}}{a_{CrO_{1.5}} X_{Mg_{0.5}AlO_2}} \quad [2]$$

The activities in the corundum phase corresponding to the tie-line compositions are obtained from the partial enthalpies and entropies, as reported by Jacob.[19]

$$\Delta G_{CrO_{1.5}} = 12,955 \, X^2_{AlO_{1.5}} + 5780 \, X^3_{AlO_{1.5}}$$
$$+ 0.9 \, RT \ln X_{CrO_{1.5}} \, J \, mol^{-1} \quad [3]$$

$$\Delta G_{AlO_{1.5}} = 21,625 \, X^2_{CrO_{1.5}} - 5780 \, X^3_{CrO_{1.5}}$$
$$+ 0.9 \, RT \ln X_{AlO_{1.5}} \, J \, mol^{-1} \quad [4]$$

The reported entropy of mixing is 0.9 times the ideal value for the solid solution with corundum structure. The integration plot is shown in Figure 7. The Gibbs–Duhem integration can be performed over the complete composition range. The value of log $\gamma_{Mg_{0.5}CrO_2}$ is given by the area below the curve with the appropriate boundary conditions. Values of log $\gamma_{Mg_{0.5}AlO_2}$ can be evaluated at any composition from the area above the curve. The derived activities for $Mg_{0.5}AlO_2$ and $Mg_{0.5}CrO_2$ in spinel solid solution at 1473 K are shown in Figure 8. Activities of both components exhibit positive deviations from Raoult's law over most of the composition range. However, the activity of $Mg_{0.5}CrO_2$ shows a small negative deviation for $Mg_{0.5}CrO_2$-rich composition; the reason for this behavior is unclear. Morita et al.[14] have measured activity of $MgCr_2O_4$ in the spinel solid solution at 1873 K by equilibrating the MgO-saturated spinel solid solution with Ni-Cr alloys under fixed oxygen partial pressures. From the measured concentration of Cr in the alloy and a separately determined value of the activity coefficient of chromium in the alloy, the activity of $MgCr_2O_4$ was calculated. Their data, after converting to $Mg_{0.5}CrO_2$ as the mixing species, are shown in Figure 8. Although the data show significant scatter, the general trend is similar to that obtained in this study, despite the considerable difference in temperature. The Gibbs energy of mixing calculated from activity
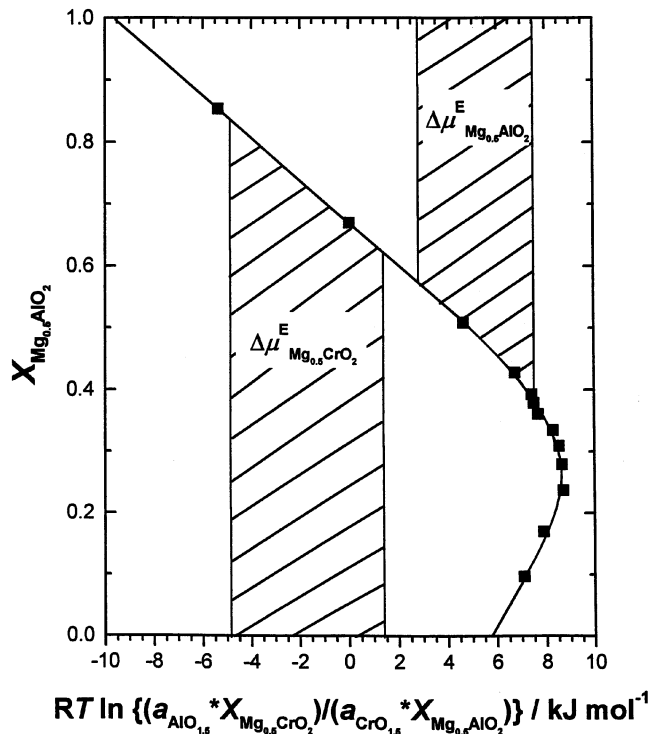
Fig. 7—Gibbs–Duhem integration plot for deriving activities for $Mg_{0.5}AlO_2$ and $Mg_{0.5}CrO_2$ from tie-line data.

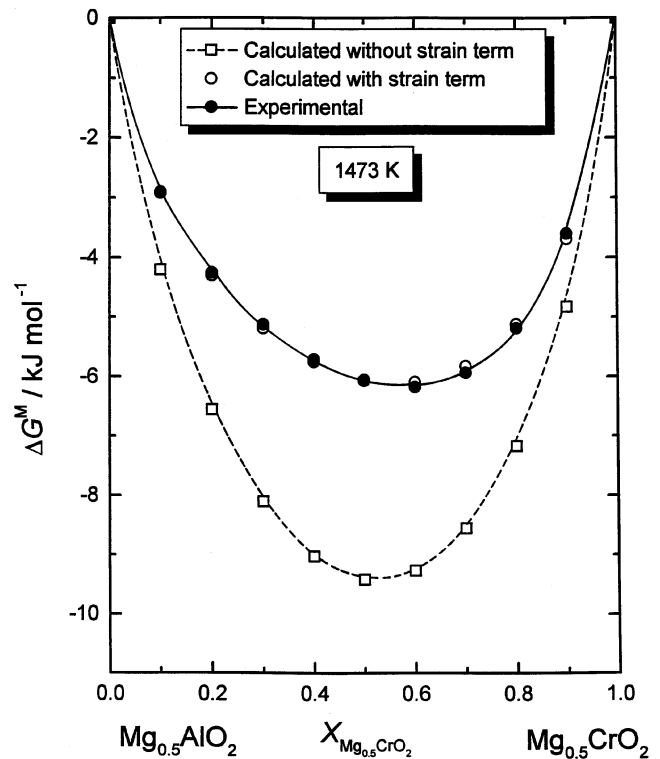Fig. 9—Comparison of the experimentally determined Gibbs energy of mixing for the system $Mg_{0.5}AlO_2$-$Mg_{0.5}CrO_2$ with the computed values based on cation distribution. The difference gives an estimate of the positive enthalpy of mixing caused by difference in radii of Al^{3+} and Cr^{3+} ions.

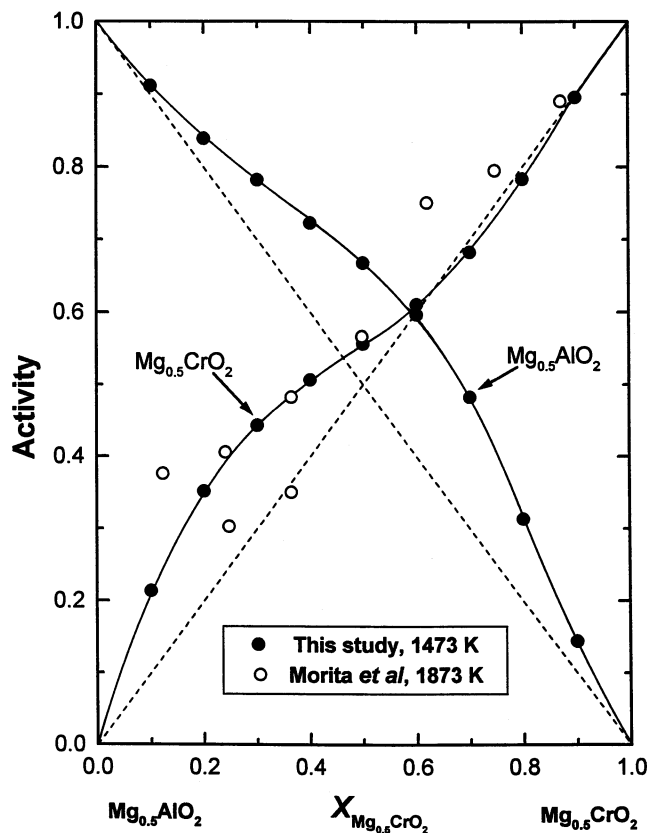Fig. 8—Activities for $Mg_{0.5}AlO_2$ and $Mg_{0.5}CrO_2$ in spinel solid solution: ——— derived from experimental data obtained in this study at 1473 K; ------ Raoult's law; and (○) data from Morita et al.[14] at 1873 K.

Table II. Activities and Gibbs Energies of Mixing in the Spinel Solid Solution $Mg_{0.5}AlO_2$-$Mg_{0.5}CrO_2$ at 1473 K Derived from Experimental Data

$X_{Mg_{0.5}CrO_2}$	$a_{Mg_{0.5}CrO_2}$	$a_{Mg_{0.5}AlO_2}$	ΔG^M (J mol^{-1})
0.0	0.0	1.0	0.0
0.1	0.213	0.912	−2903
0.2	0.352	0.839	−4257
0.3	0.443	0.782	−5124
0.4	0.506	0.723	−5711
0.5	0.556	0.667	−6069
0.6	0.611	0.597	−6175
0.7	0.683	0.483	−5936
0.8	0.784	0.314	−5185
0.9	0.896	0.144	−3599
1.0	1.0	0.0	0.0

coefficients is plotted in Figure 9 as a function of composition. The activities of components and Gibbs energy of mixing of spinel solid solution at 1473 K obtained from Gibbs–Duhem integration are listed in Table II.

The accuracy of tie-line data can be checked independently. The value of equilibrium constant and Gibbs energy change for Reaction [1] can be calculated for each tie-line, using tie-line compositions and thermodynamic data for the two solid solutions. If all the data are internally consistent, the same value for the equilibrium constant would be obtained from each tie-line. The equilibrium constant obtained from the analysis of the tie-lines is 1.227 (±0.019), where the error limit corresponds to twice the standard deviation. The corresponding standard Gibbs energy change is

$-2508 (\pm 382)$ J mol^{-1}, in excellent agreement with a value of $-2499 (\pm 570)$ J mol^{-1} obtained from direct emf measurement on MgAl$_2$O$_4$[20] and MgCr$_2$O$_4$.[21]

IV. DISCUSSION

The activity-composition relationship in the spinel solid solution can be considered in light of intracrystalline ion-exchange equilibria between cations on the tetrahedral and octahedral sites. When a transition-metal ion such as Cr^{3+} is surrounded by an octahedron of negative ions, the five d-orbitals no longer have the same energy but are split into a lower t_{2g} triplet, which is stabilized, and an upper e_g doublet, which is destabilized relative to the mean d-orbital. The same phenomenon occurs in the tetrahedral sites except that the triplet is at a higher energy than the doublet. The difference between the stabilization energies on two competing sites yields the site preference energy for a transition metal ion. The stabilization of nontransition metal ions in the nonequivalent crystallographic sites has different origins from those of transitional metal ions. Assuming orbital energy sums parallel total energies, Tossel[22] has given a qualitative explanation for the relative stability of the octahedral oxy-ions of Mg and Al over tetrahedral oxy-ions in terms of orbital binding energies obtained from X-ray emission, optical spectra, and molecular orbital calculations. The site preference energies for Mg^{2+} and Al^{3+} ions may also contain a contribution from anion polarization.

The ion-exchange equilibria between the tetrahedral and octahedral sites are governed by site preference energies of cations, as discussed by Jacob and Alcock.[23] The value for the octahedral site preference energies of Cr^{3+} was obtained by Dunitz and Orgel[24] from optical spectra using crystal field theory. Crystal field theory does not give a value for Al^{3+} ion since it has no d-electrons. The octahedral site preference energy of Al^{3+} was derived relative to that for Ni^{2+} ion from crystal field theory using the measured cation distribution in NiAl$_2$O$_4$.[25] A model based on ideal mixing of ions on each site with the inclusion of Jahn–Teller entropy for Ni^{2+} on tetrahedral site was used.[25] The site preference energy for Mg^{2+} is calculated from the experimentally determined cation distribution between tetrahedral and octahedral sites of pure MgAl$_2$O$_4$ at high temperature, as discussed subsequently.

The cation distribution in MgAl$_2$O$_4$ has been measured as a function of temperature by three groups using magic angle spinning nuclear magnetic resonance (MAS-NMR)[26,27,28] and two groups using neutron powder diffraction[29,30] techniques. The results of Millard *et al.*[26] and Maekawa *et al.*[27] are more reliable than those of Wood *et al.*,[28] since they used more appropriate instrument parameters for acquisition of[27] Al MAS-NMR spectra. The cation distribution can be described quantitatively using intracrystalline ion exchange reaction:

$$(Mg^{2+}) + [Al^{3+}] \rightarrow [Mg^{2+}] + (Al^{3+}) \qquad [5]$$
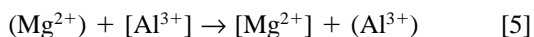
The Gibbs energy change associated with the exchange reaction (ΔG^{ex}) is zero at equilibrium:

$$\Delta G^{ex} = \Delta H^{ex} + RT \ln [\alpha^2/\{(1-\alpha)(2-\alpha)\}] = 0 \qquad [6]$$

where ΔH^{ex} is the enthalpy change for the reaction and α is the disorder parameter for pure MgAl$_2$O$_4$. The ionic fraction
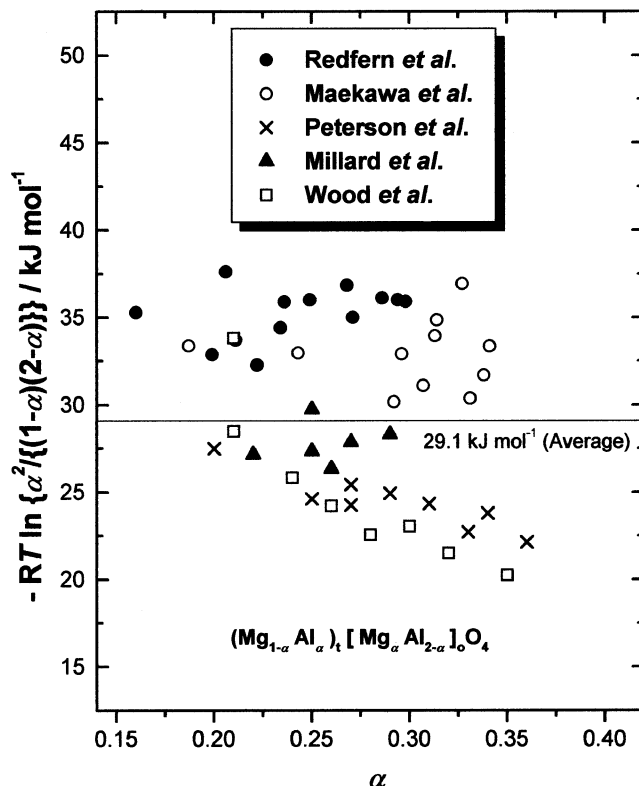

Fig. 10—Analysis of the literature data on cation distribution in MgAl$_2$O$_4$: variation of the function $-RT \ln \{\alpha^2/\{(1-\alpha)(2-\alpha)\}\}$ with α, where α is the ionic fraction of Al^{3+} in the tetrahedral sites.

of Al^{3+} on the tetrahedral site of pure MgAl$_2$O$_4$ is represented by α. Since the cation distribution in MgAl$_2$O$_4$ can be represented as $(Mg_{1-\alpha}Al_\alpha)_t [Mg_\alpha Al_{2-\alpha}]_o O_4$, α also gives the fraction of the total Mg^{2+} ions on the octahedral sites. The enthalpy change, which is equal to the difference in the octahedral site preference (osp) energies of the two cations, is related to the cation distribution:

$$\Delta H^{ex} = H^{osp}_{Mg^{2+}} - H^{osp}_{Al^{3+}} = -RT \ln [\alpha^2/\{(1-\alpha)(2-\alpha)\}] \qquad [7]$$

In this simple model, the standard entropy change for the exchange reaction is assumed to be zero. The assumption is based on the fact that the reaction is balanced both with respect to elements and sites.

The product of absolute temperature and configurational entropy change for the exchange reaction is plotted as a function of the ionic fraction of Al^{3+} ion on the tetrahedral site in Figure 10. The variation of $-RT \ln [\alpha^2/\{(1-\alpha)(2-\alpha)\}]$ with absolute temperature is displayed in Figure 11. The scatter of experimental data taken from recent publications does not warrant the use of more sophisticated models[25,31] in which the ΔH^{ex} in Eq. [7] is a function of the disorder parameter. The cation distribution in MgAl$_2$O$_4$ is adequately represented by the equation

$$-RT \ln \frac{\alpha^2}{(1-\alpha)(2-\alpha)} = 29,100 \text{ J mol}^{-1} \qquad [8]$$

Comparison of the measured cation distribution with that given by Eq. [10] is shown in Figure 12. The average value of the enthalpy change for the exchange reaction is 29.1 kJ
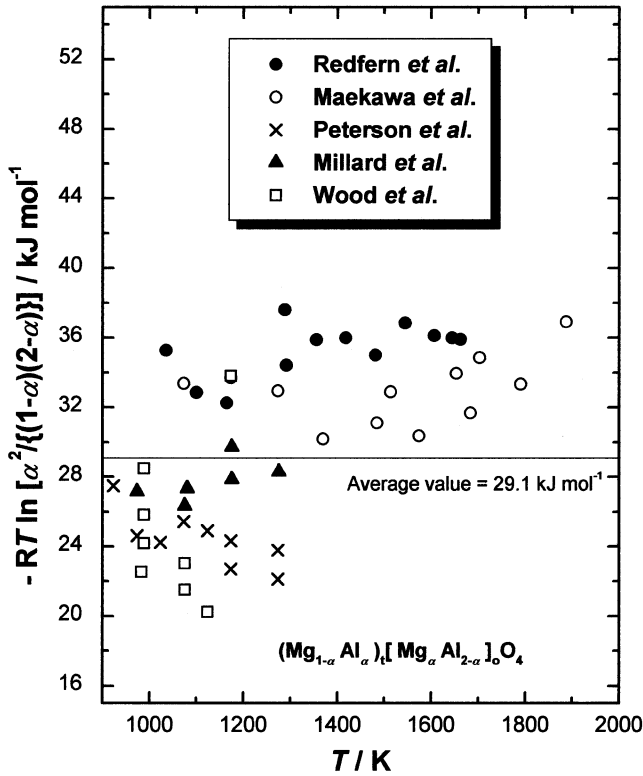
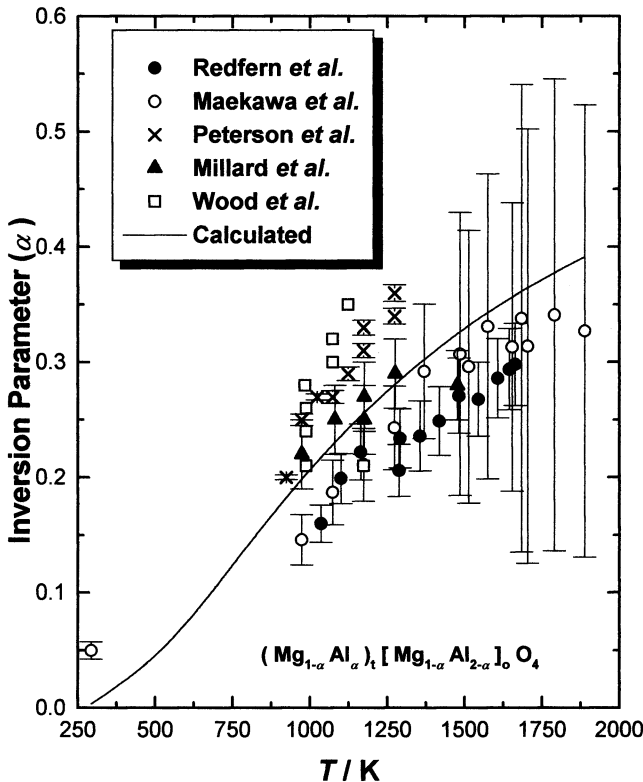Fig. 11—The temperature dependence of the function $-RT \ln \{\alpha^2/\{(1-\alpha)(2-\alpha)\}\}$ for pure MgAl$_2$O$_4$.

Fig. 12—Comparison of the measured cation distribution for pure MgAl$_2$O$_4$ with cation distribution calculated using the simple model.

METALLURGICAL AND MATERIALS TRANSACTIONS B

Table III.   Octahedral Site Preference Energies of Cations

Ion (*i*)	Octahedral Site Preference Energy (H_i^{osp}), kJ mol^{-1}	Source of Information
Mg^{2+}	−32.1	cation distribution in MgAl$_2$O$_4$ and the value for Al^{3+} (this study)
Al^{3+}	−61.2	cation distribution in NiAl$_2$O$_4$[25] and the value for Ni^{2+} from the crystal field theory[24]
Cr^{3+}	−157.7	crystal field theory[24]

mol^{-1}. From this average value, the octahedral site preference energy for Mg^{2+} ion is evaluated as −32.1 kJ mol^{-1}, relative to the value for Al^{3+} discussed previously. The octahedral site preference energies of cations used in this study are listed in Table III. Using these values, the two independent intracrystalline ion-exchange equilibria can be formulated for the spinel solid solution (Mg, Al, Cr) [Mg, Al, Cr]$_2$O$_4$:

$$(Mg^{2+}) + [Al^{3+}] \rightarrow [Mg^{2+}] + (Al^{3+}) \qquad [9]$$
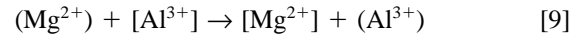
$$\Delta H^{ex} = 29{,}100 \text{ J} = -RT \ln \frac{[N_{Mg^{2+}}](N_{Al^{3+}})}{(N_{Mg^{2+}})[N_{Al^{3+}}]} \qquad [10]$$

$$(Mg^{2+}) + [Cr^{3+}] \rightarrow [Mg^{2+}] + (Cr^{3+}) \qquad [11]$$
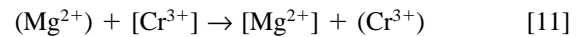
$$\Delta H^{ex} = 125{,}640 \text{ J} = -RT \ln \frac{[N_{Mg^{2+}}](N_{Cr^{3+}})}{(N_{Mg^{2+}})[N_{Cr^{3+}}]}$$
$$+ RT \ln 3 \qquad [12]$$

where round and square brackets indicate tetrahedral and octahedral sites, respectively. Mixing of cations on each sublattice is assumed to be ideal and activities of cations on each site are assumed to equal to their ionic fractions. The Cr$^{3+}(d^3$, high spin state) in the tetrahedral site produces a Jahn–Teller distortion. In the cubic phase, the direction of the distortion is randomized giving rise to an entropy contribution R ln 3 per mole. The associated mass balance equations are:

$$2[N_{Mg^{2+}}] + (N_{Mg^{2+}}) = 1 \qquad [13]$$

$$2[N_{Al^{3+}}] + (N_{Al^{3+}}) = 2X_{MgAl_2O_4} \qquad [14]$$

$$2[N_{Cr^{3+}}] + (N_{Cr^{3+}}) = 2X_{MgCr_2O_4} \qquad [15]$$

In these equations, N represents the ionic fraction of cations on each site and X represents the mole fraction of each component of the solid solution. Combining Eqs. [13] and [14] with Eq. [10], one obtains

29,100 J =
$$[16]$$
$$-RT \ln \frac{[N_{Mg^{2+}}]2\{X_{MgAl_2O_4} - [N_{Al^{3+}}]\}}{\{1 - 2[N_{Mg^{2+}}]\} [N_{Al^{3+}}]}$$

Similarly, by combining Eqs. [13] and [15] with Eq. [12], one obtains

125,640 J =
$$[17]$$
$$-RT \ln \frac{[N_{Mg^{2+}}]2\{X_{MgCr_2O_4} - [N_{Cr^{3+}}]\}}{\{1 - 2[N_{Mg^{2+}}]\}[N_{Cr^{3+}}]}$$

The sum of ionic fraction on each site is unity:

VOLUME 31B, DECEMBER 2000—1329
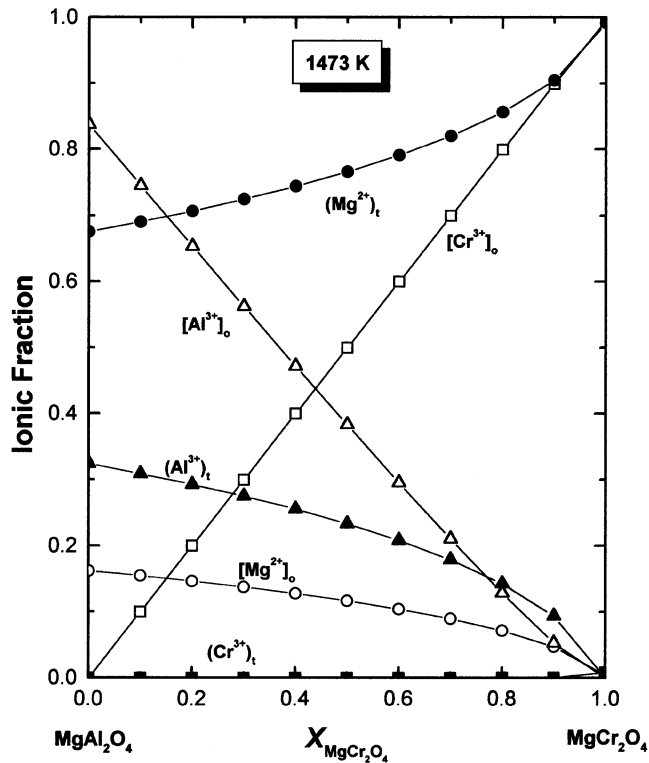
Fig. 13—Ionic fractions of cations on tetrahedral and octahedral sites of the MgAl$_2$O$_4$-MgCr$_2$O$_4$ spinel solid solution at 1473 K.

$$[N_{Mg^{2+}}] + [N_{Cr^{3+}}] + [N_{Al^{3+}}] = 1 \qquad [18]$$

$$(N_{Mg^{2+}}) + (N_{Cr^{3+}}) + (N_{Al^{3+}}) = 1 \qquad [19]$$

Using Eqs. [16], [17], and [18], the cation distribution was computed at 1473 K for different compositions of the spinel solid solution using MATLAB (Mathworks Inc., Natick, Massachusetts). The variation of cationic fractions in tetrahedral and octahedral sites with spinel composition at 1473 K is illustrated in Figure 13. Despite the difference in the octahedral site preference energies of the divalent and trivalent ions, a significant portion of Mg^{2+} ions occupy the octahedral site, especially for compositions rich in MgAl$_2$O$_4$. The variation of ionic fractions on the tetrahedral and octahedral sites with composition of the solid solution is nonlinear.

The total entropy of cation mixing on the two sites of the spinel solid solution is given by[32]

$$\Delta S_{ss}^{cm} = -R\{\Sigma(N_i) \ln (N_i)$$
$$+ 2\Sigma[N_i] \ln [N_i]\} \text{ J mol}^{-1} \text{ K}^{-1} \qquad [20]$$

The first summation on the right side represents the contribution from mixing of ions on tetrahedral sites. The second term gives contribution from mixing on the octahedral sites. There are two ions on the octahedral sites per mole of MgX$_2$O$_4$ (X = Al, Cr). The configurational entropy in a mechanical mixture of end-member components varies linearly between that for the pure components:

$$\Delta S_{mix}^{cm} = X_{MgAl_2O_4} \Delta S_{MgAl_2O_4}^{cm}$$
$$+ X_{MgCr_2O_4} \Delta S_{MgCr_2O_4}^{cm} \text{ J mol}^{-1} \text{ K}^{-1} \qquad [21]$$

Rewriting the cation mixing entropy of pure end-members

in terms of their cation disorder parameters (α for MgAl$_2$O$_4$ and β for MgCr$_2$O$_4$):

$$\Delta S_{mix}^{cm} = -R \left\{ X_{MgAl_2O_4} \left[(1 - \alpha) \ln (1 - \alpha) \right. \right.$$
$$\left. + \alpha \ln \alpha + \alpha \ln \frac{\alpha}{2} + (2 - \alpha) \ln \left(\frac{(2 - \alpha)}{2} \right) \right]$$
$$+ X_{MgCr_2O_4} \left[(1 - \beta) \ln (1 - \beta) + \beta \ln \beta \right.$$
$$\left. \left. + \beta \ln \frac{\beta}{2} + (2 - \beta) \ln \left(\frac{(2 - \beta)}{2} \right) \right] \right\} \qquad [22]$$

where β represents the ionic fraction of Cr^{3+} on the tetrahedral site of pure MgCr$_2$O$_4$. The configurational contribution to the entropy of mixing of the solid solution is obtained as the difference:

$$\Delta S^{M,cm} = \Delta S_{ss}^{cm} - \Delta S_{mix}^{cm} \text{ J mol}^{-1} \text{ K}^{-1} \qquad [23]$$

The small Jahn–Teller contribution to the mixing entropy is given by

$$\Delta S^{M,JT} = R \ln 3 \{(N_{Cr^{3+}})$$
$$- \beta X_{MgCr_2O_4}\} \text{ J mol}^{-1} \text{ K}^{-1} \qquad [24]$$

Because of the low concentration of Cr^{3+} ion in the tetrahedral site, the maximum value of $\Delta S^{M,JT}$ is 0.1 J mol^{-1}K^{-1}, small enough to be neglected. Similarly, total enthalpy of mixing caused by cation disorder can be easily computed from the fraction of trivalent ions on the tetrahedral sites.

$$\Delta H_{ss}^{cm} = (N_{Al^{3+}})_{ss} \Delta H_{MgAl_2O_4}^{ex}$$
$$+ (N_{Cr^{3+}})_{ss} \Delta H_{MgCr_2O_4}^{ex} \text{ J mol}^{-1} \qquad [25]$$

where $\Delta H_{MgAl_2O_4}^{ex} = 29,100$ Jmol^{-1} and $\Delta H_{MgCr_2O_4}^{ex} = 125,640$ J mol^{-1} are the cation exchange enthalpies for MgAl$_2$O$_4$ and MgCr$_2$O$_4$, respectively. Again, enthalpy associated with cation disorder present in a mechanical mixture of pure spinel phases is given by

$$\Delta H_{mix}^{cm} = X_{MgAl_2O_4} \alpha \Delta H_{MgAl_2O_4}^{cm}$$
$$+ X_{MgCr_2O_4} \beta \Delta H_{MgCr_2O_4}^{cm} \text{ J mol}^{-1} \qquad [26]$$

Hence, enthalpy of mixing of the solid solution is given by

$$\Delta H^{M,cm} = \Delta H_{ss}^{cm} - \Delta H_{mix}^{cm} \text{ J mol}^{-1} \qquad [27]$$

Rearranging,

$$\Delta H^{M,cm} = 29,100 \{(N_{Al^{3+}})_{ss} - \alpha X_{MgAl_2O_4}\}$$
$$+ 125,640 \{(N_{Cr^{3+}})_{ss} - \beta X_{MgCr_2O_4}\} \text{ J mol}^{-1} \qquad [28]$$

where the subscript *ss* denotes cationic fractions in the solid solution at the specified site. The Gibbs energy of mixing can be obtained by combining the enthalpy and entropy of mixing:

$$\Delta G^{M,cm} = \Delta H^{M,cm} - T(\Delta S^{M,cm} + \Delta S^{M,JT}) \text{ J mol}^{-1} \qquad [29]$$

Alternatively, activities can be obtained directly from the cation distribution using the following equations:[11]

$$a_{\text{MgAl}_2\text{O}_4} = a^2_{\text{Mg}_{0.5}\text{AlO}_2} = \frac{(N_{\text{Mg}^{2+}})[N_{\text{Al}^{3+}}]^2}{(1 - \alpha)(1 - 0.5\alpha)^2} \quad [30]$$

$$a_{\text{MgCr}_2\text{O}_4} = a^2_{\text{Mg}_{0.5}\text{CrO}_2} = \frac{(N_{\text{Mg}^{2+}})[N_{\text{Cr}^{3+}}]^2}{(1 - \beta)(1 - 0.5\beta)^2} \quad [31]$$

where the numerators on the right-hand side of the equations represent the product of ionic fractions in spinel solid solution and the denominators the corresponding product in the pure component spinels. The product of ionic fractions define the activity of each end-member component relative to the strictly normal spinel.

The Gibbs energy of mixing calculated using the simple cation-mixing model incorporating the Jahn–Teller entropy is compared with that derived from experimental tie-line data in Figure 9. In this plot, the mixing species are taken as $\text{Mg}_{0.5}\text{AlO}_2$ and $\text{Mg}_{0.5}\text{CrO}_2$. The difference between the calculated and experimental curves may be attributed to a positive enthalpy term arising from the difference in radii of Al^{3+} and Cr^{3+} ions. The Cr^{3+} ion in sixfold coordination (0.0615 nm) is considerably larger than the Al^{3+} ion (0.053 nm) according to Shannon and Prewit.[33] The size difference is slightly more on the Ahrens scale.[34] The lattice strain encountered in accommodating an ion of different size was not considered in calculating the cation distribution. Hence, it must be added as a separate term to obtain the correct value for the Gibbs energy of mixing. The strain contribution (ΔH^M_{st}) is obtained as the difference between experimental and calculated values for the Gibbs energy of mixing. The strain contribution was found to be adequately represented in the subregular model:

$$\Delta H^M_{st} = X_{\text{Mg}_{0.5}\text{AlO}_2} X_{\text{Mg}_{0.5}\text{CrO}_2} (14{,}659\, X_{\text{Mg}_{0.5}\text{AlO}_2}$$
$$+ 12{,}354\, X_{\text{Mg}_{0.5}\text{CrO}_2}) \text{ J mol}^{-1} \quad [32]$$

The contribution of the positive strain enthalpy to the Gibbs free energy of mixing become relatively more significant as temperature decreases, producing inflections in the Gibbs energy curve at lower temperatures and causing the appearance of a miscibility gap. The cation distribution, entropy, enthalpy, and Gibbs energy of mixing were calculated at various temperatures using the procedure outlined previously. The real Gibbs energy of mixing, obtained by adding the strain contribution to values calculated from cation distribution, is plotted as a function of composition in Figure 14. Inflections are seen in the Gibbs energy of mixing curves at temperatures below 800 K. The immiscibility gap boundaries are obtained using the common tangent construction. The calculated miscibility gap is shown in Figure 15. It is characterized by a critical temperature of 802 ($\pm$20) K and critical composition of $X_{\text{MgCr}_2\text{O}_4} = 0.46(\pm 0.02)$.

V. CONCLUSIONS

The tie-lines between the spinel and corundum solid solutions in ternary system $\text{MgO-Al}_2\text{O}_3\text{-Cr}_2\text{O}_3$ were accurately determined at 1473 K. The results obtained are at variance with the limited tie-line data reported by Hino et al.[15] at 1573 K. Activities in spinel solid solutions were derived from the experimental tie-line data using the modified Gibbs–Duhem integration technique of Jacob and Jeffes.[18]
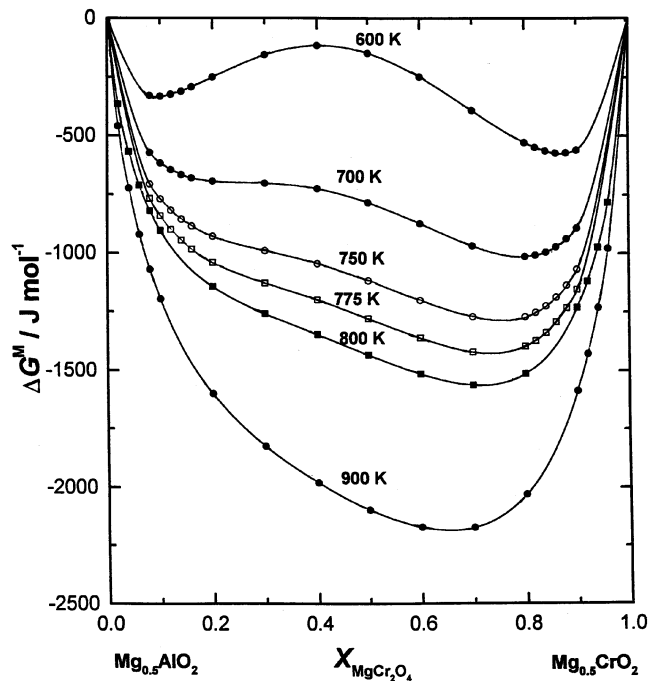

Fig. 14—Gibbs energy of mixing curves for the system $\text{Mg}_{0.5}\text{AlO}_2$-$\text{Mg}_{0.5}\text{CrO}_2$ at different temperatures. The curves at lower temperatures exhibit point of inflections and indicate phase separation.
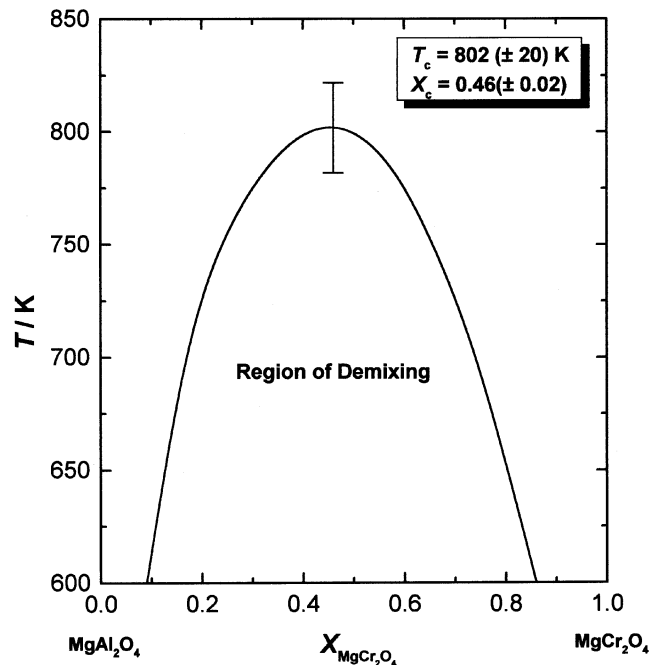

Fig. 15—Miscibility gap in the system MgAl_2O_4-MgCr_2O_4 derived from the results of this study.

Activities of $\text{Mg}_{0.5}\text{AlO}_2$ and $\text{Mg}_{0.5}\text{CrO}_2$ exhibit strong positive deviations from Raoult's law over most of the composition range. However, the activity of $\text{Mg}_{0.5}\text{CrO}_2$ exhibits mild negative deviation for compositions rich in $\text{Mg}_{0.5}\text{CrO}_2$. Activities of $\text{Mg}_{0.5}\text{CrO}_2$ obtained in this study at 1473 K are in reasonable agreement with values reported by Morita et al.[14] at 1873 K. Because the mixing occurs only on the cation sublattices, the configurational contribution to Gibbs

energy of mixing can be calculated using the strain enthalpy resulting from the difference in the radii of Al^{3+} and Cr^{3+} ions in sixfold coordination is obtained from the difference between the calculated and experimental Gibbs energy of mixing at 1473 K. A miscibility gap is predicted for the pseudobinary $MgAl_2O_4$-$MgCr_2O_4$ at temperatures below 802 ($\pm$20) K. A first-order estimate of the effect of pressure on phase relation in pseudobinary system can be obtained using volume data obtained from lattice parameter measurement: $\Delta V^M = X_{MgAl_2O_4} X_{MgCr_2O_4} (0.0423 - 0.0209 X_{MgCr_2O_4})$ J $bar^{-1} mol^{-1}$.

REFERENCES

1. T. Takaoka, Y. Kikuchi, and Y. Kawai: *Tetsu-to-Hagané*, 1990, vol. 76, pp. 1839-46.
2. S. Takeuchi, H. Nakamura, T. Sakuraya, T. Fujii, and T. Nozaki: *Tetsu-to-Hagané*, 1990, vol. 76, pp. 1847-54.
3. H. Katayama, M. Kuwabura, H. Hirata, J. Yagi, T. Saitou, and M. Fujita: *Tetsu-to-Hagané*, 1990, vol. 76, pp. 1855-62.
4. K. Taoka, C. Tada, S. Yamada, H. Nomura, M. Ohnishi, and H. Bada: *Tetsu-to-Hagané*, 1990, vol. 76, pp. 1863-70.
5. R.H. Nafziger, J.E. Tress, and J.I. Paige: *Metall. Trans. B*, 1979, vol. 10B, pp. 5-14.
6. W.J. Rankin: *Arch. Eisenhuttenwes.*, 1979, vol. 50, pp. 373-80.
7. H.G. Katayama and M. Tokuda: *Trans. Iron Steel Inst. Jpn.*, 1980, vol. 20, pp. 154-62.
8. H.G. Katayama: *Trans. Iron Steel Inst. Jpn.*, 1987, vol. 27, pp. 545-51.
9. H.G. Katayama, M. Tokuda, and M. Ohtani: *Tetsu-to-Hagané*, 1984, vol. 70, pp. 1559-65.
10. K.T. Jacob, A. Petric, G.M. Kale, and G.N.K. Iyengar: *Ceram. Int.*, 1987, vol. 13, pp. 123-29.
11. A. Petric and K.T. Jacob: *Solid State Ionics*, 1982, vol. 6, pp. 47-56.
12. K.T. Jacob and R. Patil: *Metall. Mater. Trans. B*, 1998, vol. 29B, pp. 1241-48.
13. K.T. Jacob and G.N.K. Iyengar: *Metall. Mater. Trans. B*, 1999, vol. 30B, pp. 865-71.
14. K. Morita, A. Inoue, and N. Sano: *Tetsu-to-Hagané*, 1988, vol. 74, pp. 999-1005.
15. M. Hino, K. Higuchi, T. Nagasaka, and S. Ban-ya: *Iron Steel Inst. Jpn.*, 1995, vol. 35, pp. 851-58.
16. H.T. Tsai and A. Muan: *J. Am. Ceram. Soc.*, 1992, vol. 75, pp. 1412-15.
17. D.M. Kerric and L.S. Darken: *Geochim. Cosmochim. Acta*, 1975, vol. 39, pp. 1431-38.
18. K.T. Jacob and J.H.E. Jeffes: *High Temp.-High Pressure*, 1972, vol. 4, pp. 177-82.
19. K.T. Jacob: *J. Electrochem. Soc.*, 1978, vol. 125, pp. 175-79.
20. K.T. Jacob, K.P. Jaydevan, and Y. Waseda: *J. Am. Ceram. Soc.*, 1998, vol. 81, pp. 209-12.
21. K.T. Jacob: *J. Electrochem. Soc.*, 1977, vol. 124, pp. 1827-31.
22. J.A. Tossel: *J. Phys. Chem. Solids*, 1975, vol. 36, pp. 1273-80.
23. K.T. Jacob and C.B. Alcock: *Metall. Trans. B*, 1975, vol. 6B, pp. 215-21.
24. J.D. Dunitz and L.E. Orgel: *J. Phys. Chem. Solids*, 1957, vol. 3, pp. 318-23.
25. G.N.K. Iyengar, R. Balasubramanya, and K.T. Jacob: *High Temp. Mater. Process.*, 1997, vol. 16, pp. 39-48.
26. R.L. Millard, R.C. Peterson, and B.K Hunter: *Am. Mineral.*, 1992, vol. 77, pp. 44-52.
27. H. Maekawa, S. Kato, K. Kawamura, and T. Yokokawa: *Am. Mineral.*, 1997, vol. 82, pp. 1125-32.
28. B.J. Wood, R.J. Kirkpatric, and B. Montez: *Am. Mineral.*, 1986, vol. 71, pp. 999-1006.
29. S.A.T. Redfern, R.J. Harrison, H.St.C. O'Neill, and D.R.R Wood: *Am. Mineral.*, 1999, vol. 84, pp. 299-310.
30. R.C. Peterson, G.A. Lager, and R.L Hitterman: *Am. Mineral.*, 1991, vol. 76, pp. 1455-58.
31. H.S.C. O'Neill and A. Navrotsky: *Am. Mineral.*, 1983, vol. 58, pp. 181-88.
32. K.T. Jacob and C.B. Alcock: *J. Solid State Chem.*, 1977, vol. 20, pp. 79-88.
33. R.D. Shanon and C.T. Prewitt: *Acta. Cryst.*, 1969, vol. 25B, pp. 925-45.
34. L.H. Ahrens: *Geochim. Cosmochim. Acta*, 1952, vol. 2, pp. 155-69.